

Time-Reversal-Invariant Topological Superconductivity and Majorana Kramers Pairs

Fan Zhang,* C. L. Kane, and E. J. Mele

Department of Physics and Astronomy, University of Pennsylvania, Philadelphia, Pennsylvania 19104, USA
(Received 31 December 2012; published 2 August 2013)

We propose a feasible route to engineer one- and two-dimensional time-reversal-invariant topological superconductors (SCs) via proximity effects between nodeless s_{\pm} wave iron-based SCs and semiconductors with large Rashba spin-orbit interactions. At the boundary of a time-reversal-invariant topological SC, there emerges a Kramers pair of Majorana edge (bound) states. For a Josephson π junction, we predict a Majorana quartet that is protected by mirror symmetry and leads to a mirror fractional Josephson effect. We analyze the evolution of the Majorana pair in Zeeman fields, as the SC undergoes a symmetry class change as well as topological phase transitions, providing an experimental signature in tunneling spectroscopy. We briefly discuss the realization of this mechanism in candidate materials and the possibility of using s and d wave SCs and weak topological insulators.

DOI: 10.1103/PhysRevLett.111.056402

PACS numbers: 71.10.Pm, 74.45.+c, 71.70.Ej, 74.78.Na

Introduction.—Broken symmetry and topological order are two fundamental themes of condensed-matter physics. The search for topological superconductors (SCs) [1–3] is fascinating, as gauge symmetries are spontaneously broken in the bulk, and gapless Andreev bound states (ABSs) can be topologically protected at order parameter defects, hosting Majorana fermions. Majorana fermions are immune to local noise by virtue of their nonlocal topological nature and thus give hope for fault-tolerant quantum computing [4]. The rise of topological superconductivity has been expedited by recent proposals [5–10] that hybridize ordinary SCs with helical materials, with the help of magnetic perturbations. With the use of proximity effects, electrons in a single helical band at the Fermi energy form conventional Cooper pairs, whose condensation realizes a spinless chiral p wave SC in its weak pairing regime, i.e., a topological SC with *broken* time-reversal symmetry (class D). Unique signatures, including zero bias conductance peaks, anomalous Fraunhofer patterns, and fractional Josephson effects, are starting to be observed in these systems [11–15]. A completely distinct family (class $DIII$) of time-reversal-invariant (TRI) topological SCs was proposed based on a mathematical classification of Bogoliubov–de Gennes (BdG) Hamiltonians [16–23]. $\text{Cu}_x\text{Bi}_2\text{Se}_3$ [21] and Rashba bilayers [24,25] are possible candidates; however, it seems very challenging since exotic interactions are required and experimental observations remain controversial [26–33].

A more ambitious goal is to realize TRI topological SCs *without* exotic electron-electron interactions in the *absence* of Zeeman fields. Here, we propose a feasible route to utilize proximity effect devices that combine Rashba semiconductors (RSs) and nodeless iron-based SCs. Below its transition temperature, the SC provides the RS an s_{\pm} wave spin-singlet pairing potential that switches sign between the Γ and M points [34–36]. A TRI topological SC is realized when the chemical potential is adjusted to make the inner and outer Fermi surfaces feel pairing potentials

with opposite signs. At a boundary of the 2D (1D) TRI topological SC, a Kramers pair of Majorana edge (bound) states emerge as localized midgap states. For a Josephson π junction, a Majorana quartet is protected by mirror symmetry [37], leading to a mirror fractional Josephson effect. We analyze how the Majorana pair evolves in Zeeman fields, as the SC undergoes a symmetry class change and topological phase transitions, providing an experimental signature in tunneling spectroscopy.

2D TRI topological SC.—We first introduce a minimal model on a square lattice to characterize 2D TRI SC,

$$H = -t \sum_{\langle ij \rangle, \sigma} c_{i\sigma}^{\dagger} c_{j\sigma} - i\lambda_R \sum_{\langle ij \rangle} c_{i\alpha}^{\dagger} (\boldsymbol{\sigma}_{\alpha\beta} \times \hat{\mathbf{d}}_{ij})_z c_{j\beta} + \Delta_0 \sum_i (c_{i1}^{\dagger} c_{i1}^{\dagger} + \text{H.c.}) + \Delta_1 \sum_{\langle ij \rangle} (c_{i1}^{\dagger} c_{j1}^{\dagger} + \text{H.c.}) \quad (1)$$

Here, t is the nearest neighbor hopping and $\boldsymbol{\sigma}$ are the Pauli matrices of electron spin. The second term arises from the Rashba spin-orbit interactions. Note that $\hat{\mathbf{d}}_{ij}$ is a unit vector pointing from site j to site i and we assume $\lambda_R > 0$. Δ_0 and Δ_1 , induced by the proximity effect, lead to a combined s_{\pm} wave pairing potential. It is more convenient to write the BdG Hamiltonian

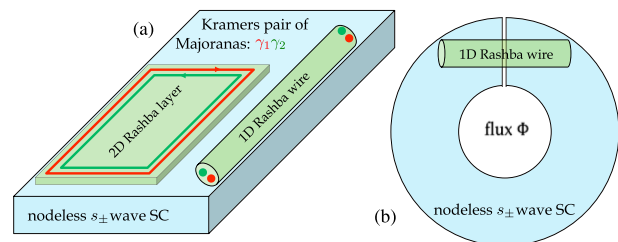


FIG. 1 (color online). (a) Sketch of the proximity devices proposed in the text. A Majorana Kramers pair emerges at the boundary when the TRI SC becomes topological. (b) Sketch of the Josephson junction described in the text.

$$\begin{aligned}\mathcal{H}_k^{\text{BdG}} &= [-2t(\cos k_x + \cos k_y) + h_k^{\text{R}} - \mu]\tau_z + \Delta_k \tau_x, \\ h_k^{\text{R}} &= 2\lambda_{\text{R}}(\sin k_x \sigma_y - \sin k_y \sigma_x), \\ \Delta_k &= \Delta_0 + 2\Delta_1(\cos k_x + \cos k_y),\end{aligned}\quad (2)$$

where μ is the chemical potential and τ are the Pauli matrices in Nambu particle-hole notation. Δ_k is a s_{\pm} wave singlet pairing potential that switches signs between the zone center $\Gamma(0,0)$ and the zone corner $M(\pi, \pi)$ when $0 < |\Delta_0| < 4\Delta_1$. As we show in Fig. 1(a) and note below, Δ_k could be provided by a nodeless iron-based SC on which the Rashba layer is deposited. $\mathcal{H}_k^{\text{BdG}}$ has time-reversal ($\Theta = -i\sigma_y K$) and particle-hole ($\Xi = \sigma_y \tau_y K$) symmetries. We obtain the energy dispersion

$$E_k^{\text{BdG}} = \pm \sqrt{[2t(\cos k_x + \cos k_y) + \mu \pm \epsilon_k^{\text{R}}]^2 + \Delta_k^2}, \quad (3)$$

where $\epsilon_k^{\text{R}} = 2\lambda_{\text{R}}\sqrt{\sin^2 k_x + \sin^2 k_y}$ is the Rashba energy. Δ_k has a closed nodal line, i.e., $\cos k_x + \cos k_y = -\Delta_0/(2\Delta_1)$, in the first Brillouin zone. At the nodal line, $E_k^{\text{BdG}} = \pm(\mu - \epsilon_0 \pm \epsilon_k^{\text{R}})$ with $\epsilon_0 = t\Delta_0/\Delta_1$, and ϵ_k^{R} has the maxima $\epsilon_{\text{max}}^{\text{R}} = 2\lambda_{\text{R}}\sqrt{2 - \Delta_0^2/(8\Delta_1^2)}$ and the minima $\epsilon_{\text{min}}^{\text{R}} = 2\lambda_{\text{R}}\sqrt{|\Delta_0/\Delta_1| - \Delta_0^2/(4\Delta_1^2)}$.

In both 2D and 1D, the \mathbb{Z}_2 topological invariant [16–19] of a TRI SC is determined by whether the pairing potential has a negative sign on odd numbers of Fermi surfaces each of which encloses a TRI momentum [18]. As shown in Fig. 2 and summarized in Table I, the phase of the hybrid SC depends on the chemical potential μ . For the case of $\epsilon_{\text{min}}^{\text{R}} \leq |\mu - \epsilon_0| \leq \epsilon_{\text{max}}^{\text{R}}$, $\mathcal{H}_k^{\text{BdG}}$ describes a nodal SC. When $|\mu - \epsilon_0| > \epsilon_{\text{max}}^{\text{R}}$, the SC is fully gapped but in the trivial ($\nu = 0$) phase since Δ_k has the same sign on both Fermi circles. When $|\mu - \epsilon_0| < \epsilon_{\text{min}}^{\text{R}}$ is satisfied, the pairing potential switches sign between the two Fermi circles, and consequently the hybrid system realizes a TRI topological SC ($\nu = 1$). The energy window for tuning the system into the $\nu = 1$ state has the size of $2\epsilon_{\text{min}}^{\text{R}}$ with an optimized value $4\lambda_{\text{R}}$ at $\Delta_0 = \pm 2\Delta_1$. For the $\nu = 1$ state, helical Majorana edge states emerge at the boundary, as shown in Fig. 2. This pair of Majorana edge states cross at $E = 0$ and $k = 0(\pi)$ for $\text{sgn}(\Delta_0/\Delta_1) = +(-)$, protected by time-reversal and particle-hole symmetries.

1D TRI topological SC.—By turning off all the k_y terms, Eq. (2) models a 1D Rashba nanowire deposited on a nodeless s_{\pm} wave SC. When the two s_{\pm} wave order parameters satisfy $|\Delta_0| < 2\Delta_1$, the pairing potential switches sign between the two TRI momenta 0 and π . In 1D, the closed nodal line of Δ_k is shrunk to two nodes at $k = \pm \arccos(-\Delta_0/2\Delta_1)$. At the nodes, the Rashba energy is $\epsilon_m^{\text{R}} = 2\lambda_{\text{R}}\sqrt{1 - \Delta_0^2/(4\Delta_1^2)}$, and thus a proximity induced 1D TRI nodal SC is identified for $\mu = \epsilon_0 \pm \epsilon_m^{\text{R}}$. When $|\mu - \epsilon_0| < \epsilon_m^{\text{R}}$, a positive pairing is induced for

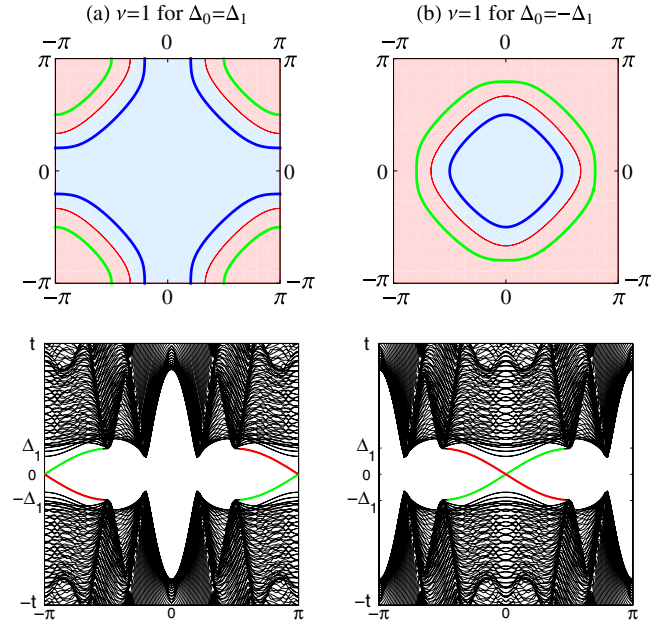


FIG. 2 (color online). Upper panels: the two Fermi surfaces (blue and green) of the single-particle bands for the $\nu = 1$ state; the closed nodal line (red) of Δ_k , separating two regions in which Δ_k has opposite signs. Lower panel: BdG spectrum of a 2D ribbon as a function of k for the $\nu = 1$ state with $\mu = \epsilon_0$. The red and green lines indicate the helical Majorana edge states. We choose parameter values $t = 10$, $\lambda_{\text{R}} = 5$, and $|\Delta_0| = \Delta_1 = 2$. (a) $\Delta_0 > 0$ and (b) $\Delta_0 < 0$.

the inner pair of Fermi points while a negative pairing is induced for the outer pair, realizing a 1D TRI topological SC. In the case of $|\mu - \epsilon_0| > \epsilon_m^{\text{R}}$, the hybrid system becomes a trivial SC that is adiabatically connected to the vacuum state.

At each end of a 1D TRI topological SC, there emerges a Kramers pair of Majorana bound states (MBSs). Without loss of generality, in the rest of this Letter we will set $\Delta_0 = 0$ for the 1D case, and thus $|\mu| < 2\lambda_{\text{R}}$ is the criterion for the $\nu = 1$ state, as shown in Fig. 3(a). The cyan line denotes four degenerate MBSs independent of Δ_1 . Further investigation of their wave functions shows that these four MBSs form two Kramers pairs localized at the opposite ends of the nanowire. This verifies our analytical results summarized in Table I. We note that the two MBSs in each Kramers pair are time-reversal partners and form a special fermion level. States with this level occupied and

TABLE I. Summary of the \mathbb{Z}_2 classification of the hybrid TRI SC in class *DIII*; ϵ_0 , ϵ_m^{R} , $\epsilon_{\text{min}}^{\text{R}}$, and $\epsilon_{\text{max}}^{\text{R}}$ are defined in the text.

Phase	Two dimension	One dimension
$\nu = 1$	$ \mu - \epsilon_0 < \epsilon_{\text{min}}^{\text{R}}$	$ \mu - \epsilon_0 < \epsilon_m^{\text{R}}$
Nodal	$\epsilon_{\text{min}}^{\text{R}} \leq \mu - \epsilon_0 \leq \epsilon_{\text{max}}^{\text{R}}$	$ \mu - \epsilon_0 = \epsilon_m^{\text{R}}$
$\nu = 0$	$ \mu - \epsilon_0 > \epsilon_{\text{max}}^{\text{R}}$	$ \mu - \epsilon_0 > \epsilon_m^{\text{R}}$

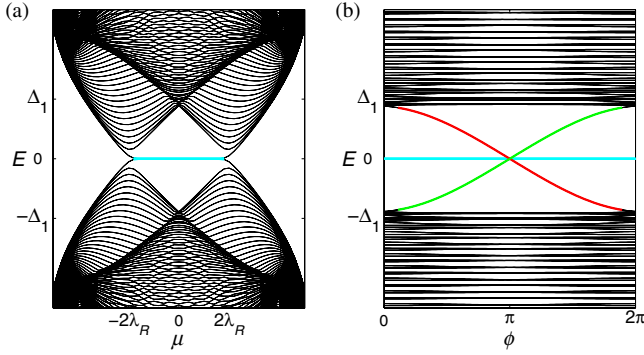


FIG. 3 (color online). (a) BdG spectrum of the 1D TRI SC as a function of μ . (b) Spectrum of ABSs in the junction as a function of ϕ . The cyan lines are fourfold degenerate, denoting two Kramers pairs of MBSs at opposite ends. The red and green lines are doubly degenerate, denoting two pairs of ABSs in the junction. We choose parameter values $t = 10$, $\lambda_R = 5$, $\Delta_1 = 2$, and $\Delta_0 = 0$; $\mu = 0$ is used in (b).

unoccupied are time-reversal partners, and thus time-reversal symmetry acts like a supersymmetry that changes the fermion parity.

Mirror fractional Josephson effect.—Consider the linear Josephson junction in Fig. 1(b), in which a Rashba nanowire is deposited on a larger s_{\pm} wave SC ring, and the phase difference $\phi = (2e/\hbar)\Phi$ across the junction is controlled by the magnetic flux Φ through the ring. Figure 3(b) shows the spectrum of ABSs as a function of ϕ when the physical separation between the ends of the SC ring is small. The fourfold cyan line shows the appearance of a pair of MBSs at each end of the wire. The red and green lines, both doubly degenerate, represent two pairs of ABSs in the junction. When $\phi \neq \pi$, time-reversal symmetry is broken and a finite μ lifts the degeneracy. However, protected by particle-hole, time-reversal, and mirror ($\mathcal{M}_y = -i\sigma_y$) symmetries [37], their crossing at $E = 0$ and $\phi = \pi$ is a fourfold degeneracy of special significance. This π junction is in sharp contrast with its \mathbb{Z}_2 counterpart in the class without mirror symmetry [9,19,38]. Splitting the Majorana quartet at $\phi = \pi$ requires breaking mirror or time-reversal symmetry [37].

To further understand this topological twist, we linearize our model (2) near the Fermi energy to

$$\mathcal{H}_{\text{eff}} = (vk_x\sigma_y - c)s\tau_z - \mu\tau_z + \mathcal{H}_{\text{SC}}, \quad (4)$$

$$\mathcal{H}_{\text{SC}} = \Delta s \left[\cos\frac{\phi}{2}\tau_x + \text{sgn}(x)\sin\frac{\phi}{2}\tau_y \right], \quad (5)$$

where $s = \pm$ denote the inner and outer bands with opposite spin helicities and c ($0 < c < \mu$) lifts their degeneracy. We find the ABS dispersions $\epsilon_s(\phi) = \Delta \cos(\phi/2)$. Note that the perfect normal state transmission and the independence on μ , c , and s are artifacts of the simplified model. We can define Bogoliubov operators $\Gamma_{s\pm}$ that satisfy

$\Gamma_s \equiv \Gamma_{s+} = \Gamma_{s-}^{\dagger}$ because of the particle-hole symmetry. The low-energy Hamiltonian is thus $H = \sum_s \epsilon_s(\phi) [\Gamma_s^{\dagger} \Gamma_s - (1/2)] = 2i \sum_s \epsilon_s(\phi) \gamma_s \eta_s$ where $\gamma_s = (\Gamma_s^{\dagger} + \Gamma_s)/2$ and $\eta_s = i(\Gamma_s^{\dagger} - \Gamma_s)/2$ are the Majorana operators. The mirror symmetry allows one to label the bands with the eigenvalues of σ_y . For each s , $\Gamma_s^{\dagger} \Gamma_s = 0, 1$ distinguishes two states with different mirror eigenvalues, and coupling them requires a process that changes $\Gamma_s^{\dagger} \Gamma_s$. Because of the Cooper pairing, the total charge is not conserved. However, the fermion parity $\Gamma_s^{\dagger} \Gamma_s$ is conserved, as the mirror symmetry does not allow scattering between the two bands. This mirror fermion parity conservation forbids the mixing of the four ABSs in the junction and therefore protects their crossing at zero energy.

The phase difference ϕ acts like a defect and parametrizes the mirror fermion parity pump. Although Eq. (4) is invariant under $\delta\Phi = h/2e$, the global Hamiltonian is physically distinct. When a flux $h/2e$ is threaded through the SC ring, ϕ is advanced by 2π , $\gamma_s \rightarrow \gamma_s$ while $\eta_s \rightarrow -\eta_s$, and a unit of fermion parity is transferred between the two bands resolving the fermion parity anomaly for an individual band. In response to the phase change, the populated ABSs carry supercurrents $I_{s\pm} = \pm I_s$, whereas the states in the continuum have negligible contributions. We obtain $I_s = (e/\hbar)\partial\epsilon_s/\partial\phi \sim \sin(\phi/2)$, which is maximized at $\phi = \pi$ in sharp contrast to the $\nu = 0$ (conventional) case. In the absence of mirror symmetry breaking, there is no transition among $I_{s\pm}$, signaling a mirror fractional Josephson effect with 4π periodicity.

Evolution of Majorana pair in Zeeman field.—When one helical band is removed from the Fermi energy, a Rashba nanowire proximity coupled to an s wave SC is a topological SC with broken-time-reversal symmetry, supporting a single MBS at each end. Since only one band is present at the Fermi energy, this also occurs even if the SC is s_{\pm} wave. Realizing such a topological phase requires μ and a Zeeman field $V_z\sigma_z$ (or $V_z\sigma_x$) to satisfy $4\Delta_1^2 + (|\mu| - 2t)^2 < V_z^2 < 4\Delta_1^2 + (|\mu| + 2t)^2$, provided that the hybrid SC remains fully gapped ($\mu^2 \neq 4\lambda_R^2 + V_z^2$). The latter condition is guaranteed for the TRI $\nu = 1$ phase as it satisfies $|\mu| < 2\lambda_R$. It is thus intriguing to investigate how the Majorana pair evolves in the Zeeman field, as the bulk SC undergoes a symmetry class change and topological phase transitions. Figure 4(a) shows the evolution in the case of $\mu \neq 0$. When V_z is turned on, without gap closing, the topological SC in the TRI class becomes a trivial SC in the class without time-reversal symmetry. Two topological phase transitions occur at $V_z^2 = 4\Delta_1^2 + (|\mu| \pm 2t)^2$ where the gap closes. The $\nu = 1$ state in the new class is realized between the transitions. At one end, as V_z is tuned up, one MBS disappears at the first transition while the other persists in the $\nu = 1$ state and enters the bulk continuum at the second transition. For the special case $\mu = 0$, the two transitions merge into one and the new $\nu = 1$ state does not appear.

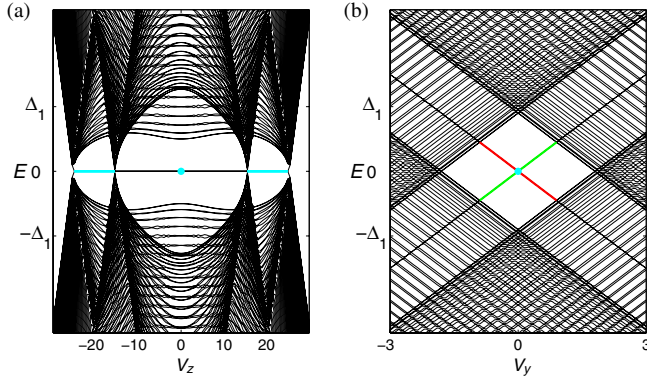


FIG. 4 (color online). Evolution of a MBS pair in Zeeman fields. (a) In a σ_z (σ_x) field; (b) in a σ_y field. The cyan dots (lines) have twofold (no) degeneracy, indicating the appearance of a MBS pair (single MBS) at the end of the SC. The black lines at zero energy are doubly degenerate. The red and green lines indicate the Zeeman splitting of two zero-energy states with opposite fermion parity. We choose parameter values $\mu = -5$ in (a) and $\mu = 0$ in (b), and the others are the same as in Fig. 3.

As implied by the zero-energy black lines in Fig. 4(a), it seems baffling that the Majorana pair is robust against the Zeeman field before the first transition occurs. We emphasize that these Majorana pairs are not topologically protected because the bulk SC is trivial in the new class. However, their robustness can be understood using the effective model described by Eq. (4) with

$$\mathcal{H}_{\text{SC}} = \Delta s \tau_x \theta(a - |x|) + \bar{\Delta} \tau_x \theta(|x| - a), \quad (6)$$

where $x = \pm a$ are the locations of the two ends of SC and $\bar{\Delta} \rightarrow \infty$ reflects the infinity mass of vacuum. Equation (6) incorporates the correct boundary condition [39] of a TRI topological SC. Solving the boundary problem, we find that a pair of MBSs at one end forms two states with $\sigma_y = \tau_y = \pm 1$ whereas the other pair at the opposite end forms two states with $\sigma_y = -\tau_y = \pm 1$. Clearly, a σ_x or σ_z Zeeman field only couples states with opposite σ_y flavors at opposite ends, whose wave function overlap decays exponentially on the SC length. Consequently, none of the Majorana pairs can be passivated away from zero energy until the first topological phase transition [40]. However, as shown in Fig. 4(b), a small σ_y field can Zeeman split the two zero-energy states with opposite fermion parity at each end, revealing the topological triviality of bulk SC. The σ_y field also closes the SC gap.

The evolution of a Majorana pair in a Zeeman field provides a “smoking gun” for the identification of a TRI topological SC in tunneling spectroscopy. In a single-channel quantum point contact, the Majorana pair induces resonant Andreev reflection producing a quantized zero bias conductance peak [41–43] of $4e^2/h$. This peak

persists for small σ_x and σ_z fields, reduces to $2e^2/h$ after the first topological quantum phase transition, and disappears at the second one. In contrast, a small σ_y field not only Zeeman splits but also reduces the peak.

Discussion.—Unlike a d_{xy} wave SC, where it is impossible to induce a full gap at the Fermi surface centered at a TRI momentum, an s_{\pm} or $d_{x^2-y^2}$ wave SC allows the pairing potentials on Fermi surfaces centered at $(0, 0)$ and (π, π) or at $(0, \pi)$ and $(\pi, 0)$ to have opposite signs. Thus, it is possible to build a 2D TRI topological SC by hybridizing a weak topological insulator with two surface states and an s_{\pm} or $d_{x^2-y^2}$ wave SC (Supplemental Material [44]). Although rotational symmetry of RS makes a hybrid 2D $d_{x^2-y^2}$ wave SC nodal, it is possible to use them to engineer a 1D TRI topological SC, as suggested by Wong and Law [45]. One might wonder whether it is possible to utilize a pure s wave SC. We note that this seems implausible (Supplemental Material [44]).

Our proposal is experimentally feasible, since the necessary ingredients and required technologies are all well established. It has been widely accepted that, at least for iron pnictides, there is a large family of nodeless s_{\pm} wave SCs [34–36], though their pairing mechanism is still under lively debate. An iron pnictide with closer electron and hole Fermi surfaces is preferred. $\Delta_{0,1}$ can be adjusted by doping or changing materials. Iron pnictides consist of square layers that are stacked in tetragonal structures, and it is better to choose a RS with cubic or tetragonal structures, e.g., Au, Ag, and Pb [46]. Small lattice incommensurability may blur and effectively broaden the induced pair potential in RSs, which may be helpful as long as the hybrid SC remains nodeless.

Our proposal for the realization of TRI topological SCs in 1D and 2D constitutes six critical advances: (i) there is no need for magnetic perturbations or exotic interactions, simplifying the experimental setup; (ii) the SC gap can reach more than 15 meV, raising the critical temperature of topological SCs; (iii) the time-reversal symmetry likely provides an Anderson’s theorem to mitigate the role of bulk disorder, making the superconductivity more robust; (iv) irrelevant bands are absent and higher subbands play no role [47], allowing large tunability in feasible materials; (v) the chemical potential is not necessarily close to the band degeneracy point of RS, where the electron density is low and the disorder effect is large; and (vi) the Majorana pairs are stable to pair fluctuations, as long as the fluctuations neither close the gap nor change the pairing sign at any Fermi surface. Our work also provides a way to use the presence of Majorana fermions to test the pairing symmetry of unconventional SCs.

This work was supported by DARPA Grant No. SPAWAR N66001-11-1-4110. C. L. K. was supported by NSF Grant No. DMR 0906175 and a Simons Investigator award from the Simons Foundation.

*zhf@sas.upenn.edu

- [1] N. Read and D. Green, *Phys. Rev. B* **61**, 10267 (2000).
- [2] D. A. Ivanov, *Phys. Rev. Lett.* **86**, 268 (2001).
- [3] A. Kitaev, *Phys. Usp.* **44**, 131 (2001); *Ann. Phys. (N.Y.)* **303**, 2 (2003).
- [4] C. Nayak, S. H. Simon, A. Stern, M. Freedman, and S. Das Sarma, *Rev. Mod. Phys.* **80**, 1083 (2008).
- [5] L. Fu and C. L. Kane, *Phys. Rev. Lett.* **100**, 096407 (2008).
- [6] M. Sato, Y. Takahashi, and S. Fujimoto, *Phys. Rev. Lett.* **103**, 020401 (2009).
- [7] J. D. Sau, R. M. Lutchyn, S. Tewari, and S. Das Sarma, *Phys. Rev. Lett.* **104**, 040502 (2010).
- [8] J. Alicea, *Phys. Rev. B* **81**, 125318 (2010).
- [9] R. M. Lutchyn, J. D. Sau, and S. Das Sarma, *Phys. Rev. Lett.* **105**, 077001 (2010).
- [10] Y. Oreg, G. Refael, and F. von Oppen, *Phys. Rev. Lett.* **105**, 177002 (2010).
- [11] V. Mourik, K. Zuo, S. M. Frolov, S. R. Plissard, E. P. A. M. Bakkers, and L. P. Kouwenhoven, *Science* **336**, 1003 (2012).
- [12] M. T. Deng, C. L. Yu, G. Y. Huang, M. Larsson, P. Caroff, and H. Q. Xu, *Nano Lett.* **12**, 6414 (2012).
- [13] M. Veldhorst, M. Snelder, M. Hoek, T. Gang, V. K. Guduru, X. L. Wang, U. Zeitler, W. G. van der Wiel, A. A. Golubov, H. Hilgenkamp, and A. Brinkman, *Nat. Mater.* **11**, 417 (2012).
- [14] J. R. Williams, A. J. Bestwick, P. Gallagher, S. S. Hong, Y. Cui, A. S. Bleich, J. G. Analytis, I. R. Fisher, and D. Goldhaber-Gordon, *Phys. Rev. Lett.* **109**, 056803 (2012).
- [15] L. P. Rokhinson, X. Liu, and J. K. Furdyna, *Nat. Phys.* **8**, 795 (2012).
- [16] A. P. Schnyder, S. Ryu, A. Furusaki, and A. W. W. Ludwig, *Phys. Rev. B* **78**, 195125 (2008).
- [17] A. Kitaev, *AIP Conf. Proc.* **1134**, 22 (2009).
- [18] X. L. Qi, T. L. Hughes, and S. C. Zhang, *Phys. Rev. B* **81**, 134508 (2010).
- [19] J. C. Y. Teo and C. L. Kane, *Phys. Rev. B* **82**, 115120 (2010).
- [20] X. L. Qi, T. L. Hughes, S. Raghu, and S. C. Zhang, *Phys. Rev. Lett.* **102**, 187001 (2009).
- [21] L. Fu and E. Berg, *Phys. Rev. Lett.* **105**, 097001 (2010).
- [22] M. Sato, *Phys. Rev. B* **81**, 220504(R) (2010).
- [23] S. Nakosai, J. C. Budich, Y. Tanaka, B. Trauzettel, and N. Nagaosa, *Phys. Rev. Lett.* **110**, 117002 (2013).
- [24] S. Nakosai, Y. Tanaka, and N. Nagaosa, *Phys. Rev. Lett.* **108**, 147003 (2012).
- [25] S. Deng, L. Viola, and G. Ortiz, *Phys. Rev. Lett.* **108**, 036803 (2012).
- [26] Y. S. Hor, A. J. Williams, J. G. Checkelsky, P. Roushan, J. Seo, Q. Xu, H. W. Zandbergen, A. Yazdani, N. P. Ong, and R. J. Cava, *Phys. Rev. Lett.* **104**, 057001 (2010).
- [27] L. A. Wray, S. Y. Xu, Y. Xia, Y. S. Hor, D. Qian, A. V. Fedorov, H. Lin, A. Bansil, R. J. Cava, and M. Z. Hasan, *Nat. Phys.* **6**, 855 (2010).
- [28] S. Sasaki, M. Kriener, K. Segawa, K. Yada, Y. Tanaka, M. Sato, and Y. Ando, *Phys. Rev. Lett.* **107**, 217001 (2011).
- [29] T. Kirzhner, E. Lahoud, K. B. Chaska, Z. Salman, and A. Kanigel, *Phys. Rev. B* **86**, 064517 (2012).
- [30] X. Chen, C. Huan, Y. S. Hor, C. A. R. Sá de Melo, and Z. Jiang, [arXiv:1210.6054](https://arxiv.org/abs/1210.6054).
- [31] N. Levy, T. Zhang, J. Ha, F. Sharifi, A. A. Talin, Y. Kuk, and J. A. Stroscio, *Phys. Rev. Lett.* **110**, 117001 (2013).
- [32] B. J. Lawson, Y. S. Hor, and Lu Li, *Phys. Rev. Lett.* **109**, 226406 (2012).
- [33] H. Peng, D. De, B. Lv, F. Wei, and C. Chu [Phys. Rev. B (to be published)].
- [34] K. Ishida, Y. Nakai, and H. Hosono, *J. Phys. Soc. Jpn.* **78**, 062001 (2009).
- [35] I. I. Mazin, *Nature (London)* **464**, 183 (2010).
- [36] T. Das and A. V. Balatsky, *J. Phys. Condens. Matter* **24**, 182201 (2012).
- [37] F. Zhang, C. L. Kane, and E. J. Mele, following Letter, *Phys. Rev. Lett.* **111**, 056403 (2013).
- [38] L. Fu and C. L. Kane, *Phys. Rev. B* **79**, 161408(R) (2009).
- [39] F. Zhang, C. L. Kane, and E. J. Mele, *Phys. Rev. B* **86**, 081303(R) (2012).
- [40] Alternatively, one can think that the Hamiltonian with a σ_x or σ_z Zeeman field has an effective time-reversal symmetry ($\Theta = K$) and thus belongs to the BDI symmetry class with an integer classification. $\tau_y \sigma_y = \Theta \Xi$ is the new chiral symmetry operator and our state is topological ($\nu = 2$) in this new symmetry class.
- [41] K. T. Law, P. A. Lee, and T. K. Ng, *Phys. Rev. Lett.* **103**, 237001 (2009).
- [42] M. Wimmer, A. R. Akhmerov, J. P. Dahlhaus, and C. W. J. Beenakker, *New J. Phys.* **13**, 053016 (2011).
- [43] For a review, see: C. W. J. Beenakker, *Annu. Rev. Condens. Matter Phys.* **4**, 113 (2013).
- [44] See the Supplemental Material at <http://link.aps.org/supplemental/10.1103/PhysRevLett.111.056402> for more discussions on the possibility of using s and d wave SCs and weak topological insulators to build TRI topological SCs.
- [45] C. L. M. Wong and K. T. Law, *Phys. Rev. B* **86**, 184516 (2012).
- [46] For the 2D case, the thin film is best grown along the (001) direction to utilize the square symmetry; (111) thin films with hexagonal symmetry may require a large λ_R value. For the 1D case, either growing direction works.
- [47] The bulk bands [5] or the band removed from Fermi energy [7–10] play negative roles in realizing a class D topological SC experimentally. There are no such problems in our case. Furthermore, the topological criterion in class $DIII$ only cares about the sign of pairing potential at Fermi surfaces, implying that higher subbands not present at Fermi energy play no role.